Pfändler *et al. J Infrastruct Preserv Resil* (2022) 3:17
https://doi.org/10.1186/s43065-022-00064-3

Journal of Infrastructure Preservation and Resilience

RESEARCH Open Access

Inspecting the corrosion state of underground reinforced concrete structures

Patrick Pfändler*, Lukas Bircher and Ueli Angst

Abstract

Unnoticed corrosion in underground reinforced concrete structural members – such as foundations, retaining walls, or piles – may severely threaten the integrity of structures. However, condition assessment of the ground-buried structural parts is challenging, because the areas of interest are hardly accessible for visual inspection or non-destructive testing. An example of particular practical relevance is reinforcement corrosion at the back-side of the lower end of cantilever retaining walls, near the construction joint between stem and heel of the base slab. The collapse of a cantilever retaining wall in Austria was a tragic reminder of the dangers of unnoticed corrosion. The drawback of current inspection methods is that they are laborious and costly, but still, only a tiny fraction of the structure can be inspected. Considering that the degree of corrosion can vary significantly along a structure, such local information includes a risk that corrosion elsewhere remains undetected.

A novel inspection system is proposed here, combining the well-proven half-cell potential measurement technique with steered horizontal underground drilling technologies. With this approach, a tailor-made probe is brought in proximity to the concrete surface in the soil and electrochemical measurements are performed to characterize the corrosion condition. The main advantage is that virtually the entire length of the structure can be inspected, thus overcoming the limitations of highly local inspection. Moreover, the proposed technique includes a method to constantly monitor the functionality of the potential measuring probe, based on electrical resistance measurements. The feasibility of the approach was confirmed in laboratory experiments on a mortar block in soil. These findings were confirmed in a field experiment. The results suggest that local corroding zones of practice-relevant size can be detected for a distance between the reference electrode and the steel surface of at least 25 cm. On the basis of this work, underground corrosion inspection of cantilever retaining walls is considered feasible, and the development of similar technologies as the one proposed here may in the future considerably enhance condition assessment of structures buried in the ground.

Keywords: Corrosion, Inspection, Reinforced concrete, Underground, Non-destructive testing, Half-cell potential mapping, Retaining wall, Foundation

Introduction

Importance of corrosion inspection of buried structural members made with reinforced concrete

Underground parts of civil engineering structures are often made of reinforced concrete (RC). This is because of the generally good corrosion resistance of RC in soil and rock environment compared to other structural materials such as steel or wood. The alkaline concrete surrounding the steel ensures passivity and, thus, negligibly low corrosion rates [1]. Nevertheless, different causes can still lead to steel corrosion in underground RC. For instance, if the steel is locally not entirely surrounded by concrete, e.g., due to structural cracks, delaminations, honeycombs, or too low cover depths, the exposed steel is at high risk for corrosion in most soil environments [2]. These environments are typically characterised by

*Correspondence: patrick.pfaendler@ifb.baug.ethz.ch
Institute for Building Materials, ETH Zürich, Zürich, Switzerland

near-neutral pH conditions and the presence of moisture and corrosive species such as chloride ions or carbonate species, which can lead to significant anodic dissolution rates. This situation is generally aggravated by the formation of galvanic elements within the structure, which can arise when the exposed steel, behaving as the anode, is in electrical contact with cathodically acting reinforcing steel, namely steel in alkaline, potentially even well-aerated (near-surface) concrete. Galvanic elements with a large cathodic area with respect to relatively small anodic zones promote high local corrosion rates at the exposed anodic site. Additionally, the soil in contact with the underground RC member provides an electrolyte through which the galvanic current can easily flow. All these factors can lead to relatively high rates of local corrosion in the zones where the reinforcing steel is not well surrounded by concrete.

A particular challenge associated with such underground corrosion situations is that there are limited options to inspect these structural members [3]. Inspecting underground structures is generally difficult due to a lack of accessibility since parts of the structure are covered with soil or other backfill materials. Thus, the detection of corrosion in underground RC members can be challenging. Unnoticed corrosion may severely threaten the integrity of such structures. Cantilever retaining walls are examples of structures where unnoticed corrosion of the underground part can lead to catastrophic failures. A RC cantilever wall collapsed in Austria without prior warning and, sadly, caused a casualty [4–6]. By now, it is well documented that the reinforcing steel at the lower end of the backside (facing the soil) of cantilever retaining walls near the foundation can corrode. This corrosion-related problem can be explained by inappropriate construction practices approximately 50 years ago [5] when many of the currently still existing retaining walls were built. During construction, insufficient quality control increased the risk of gaps and honeycombs at the joint between the foundation and the wall, leaving the reinforcing steel exposed directly to the soil or backfill environment [7]. Corrosion at this location presents a twofold problem: First, as mentioned above, inspecting this part of the structure is virtually impossible (or can only be done as random spot-checks with high inspection costs). Second, this location in the structure is often the most critical, as corrosion-related degradation of the reinforcing steel in this section can cause sudden wall failure [5, 8] or increase the risk of such a failure [9].

A report by Switzerland's federal roads office (FEDRO) published in 2016 mentioned that their infrastructure stock has 500 cantilever retaining walls in a so-called critical condition [10]. These numbers do not include the walls owned by cantons or municipalities in Switzerland. It can also be assumed that other countries will have a considerable amount of cantilever retaining walls and are going to face similar challenges [10]. In order to tackle the safety aspects and the financial consequences associated with cantilever retaining walls, FEDRO analysed maintenance works from such walls from several projects [6] with varying ages between 35 and 47 years. The focus was on the steel reinforcement in the joint between the foundation and the wall. A total of 1821 individual steel bars were checked at 259 sections of such walls from four different national roads. The main findings were that 24% of all steel bars showed corrosion-related damages and that 42% of the elements had steel bars with corrosion damages. Similar findings, namely the high variability of the condition, were also reported by others, e.g. Tremblay et al. for RC vaults [11] or by Rebhan et al. for cantilever retaining walls [12]. This brief analysis highlights the importance of spatially distributed measurements in the form of line or area measurements to consider the varying degree of corrosion damage in RC structures [6, 11, 12].

The common practice of inspection can be divided into destructive testing and non-destructive testing methods, of which several were examined in the literature for the applicability to buried structural members, especially for retaining walls [6, 11–14], particularly the inspection of the reinforcement on the backside. Ultrasonic or radar waves may detect large corrosion spots and honeycombs, but the detectability depends on several boundary conditions [15]. Monitoring systems with inclinometers and reflectors detect geotechnical problems such as sliding or tipping of the wall but are not suitable for corrosion detection [12]. A novel system for monitoring applies a new combination of sensors (strain gauges and inclinometers) placed at different heights in order to distinguish between effects caused by temperature changes or by ongoing corrosion of the reinforcement at the backside [12]. This might lead to continuous monitoring. Material qualities and wall geometry restrict the study's applicability to other retaining walls.

In Switzerland, the backside of the cantilever retaining wall is often inspected with three methods [5]. Figure 1 (A) to (C) present all three inspection methods, namely (A) excavating a shaft behind the retaining wall, (B) (ultra)high-pressure water jetting of the wall from an excavated part in the front, and (C) core drillings through the entire wall from the front side. The common goal of all inspection methods is to locate corroded steel at the backside between the foundation and the wall [5, 6]. All three methods offer different advantages and disadvantages considering the required time and space needed for the inspection, the inspection costs, the implications

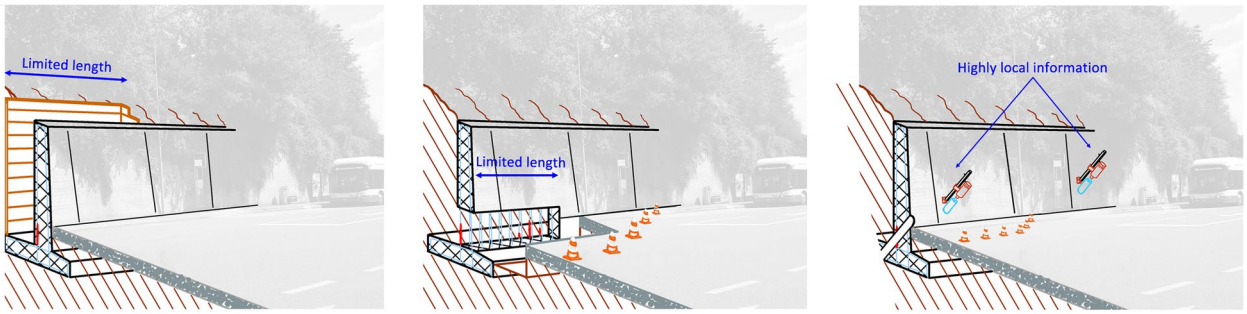

Fig. 1 Current inspection methods for RC retaining walls. The corrosion damage is marked in red at the backside of the wall: **A** Excavation of backfill, followed by concrete cover removal and visual inspection of the corrosion state from the backside; **B** Removal of concrete with hydro-jetting and visual inspection of the corrosion damage from the front side; **C** Extraction of drilling cores from the front side for analysis in the laboratory

regarding the transport of the backfill material or the removal of the structurally relevant steel bars, or the impact on the traffic in the form of caused traffic jams or blocked lanes. Furthermore, it is well-known that the degree of damage can vary even by comparing neighbouring steel bars in the working joint of those walls [5, 6]. Despite this knowledge, the current inspection methods have in common that only a small fraction of the structure's length is inspected. As reinforcement corrosion can occur in a spatially limited area, the risk for misclassification of the corrosion condition of the retaining wall is relatively high since the consulting engineer often needs to conclude the condition and safety of the whole wall based on limited information derived from these inspections. On the one hand, this can lead to unnecessary costly repairs; on the other hand, it might cause an increased risk of failure [5, 6].

Development of an underground inspection probe

Concept

This paper presents a novel approach for the non-destructive condition assessment of buried structural parts made with RC. The well-proven half-cell potential (HCP) mapping technique is combined with a novel underground inspection probe and directed horizontal drilling technology. Figure 2 shows the concept of the inspection method where the inspection probe moves inside a micro-tunnel along the backside of the wall, preferably at the height of the construction joint and laterally close to it. This micro-tunnel is created utilizing horizontal drilling technology. The probe should deduct information about the corrosion state of the steel reinforcement.

The underground inspection probe needs to fulfil several requirements regarding the out-of-sight measurement of the HCP mapping and the prevention of damage during transport between the measurement locations in the underground. The independence between the construction of the micro-tunnel and the corrosion inspection allows for splitting the two processes temporarily. Existing horizontal drilling technology allows creating of micro-tunnels in various soil compositions, whereas a probe suitable for underground corrosion inspection does not exist. Furthermore, horizontal drilling technologies can be steered with a radius dependent on the equipment that itself depends mainly on the filling material behind the retaining wall. The steering allows following curved retaining walls or correcting minor deviations from the desired path towards the necessary excavation at the other lateral end of the wall. The main focus of this work was to develop and test such a novel probe that can be moved through a micro-tunnel and allows the

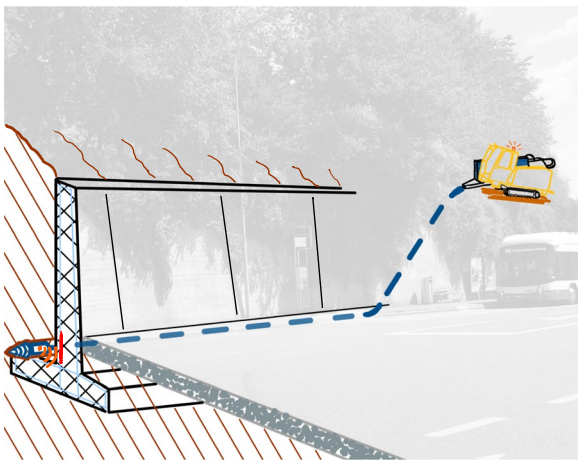

Fig. 2 Concept of the underground inspection method with directed horizontal drilling methods for retaining wall along the working joint where the suspected region for reinforcement corrosion is marked in red. Ideally, the inspection does not affect the traffic lanes nearby

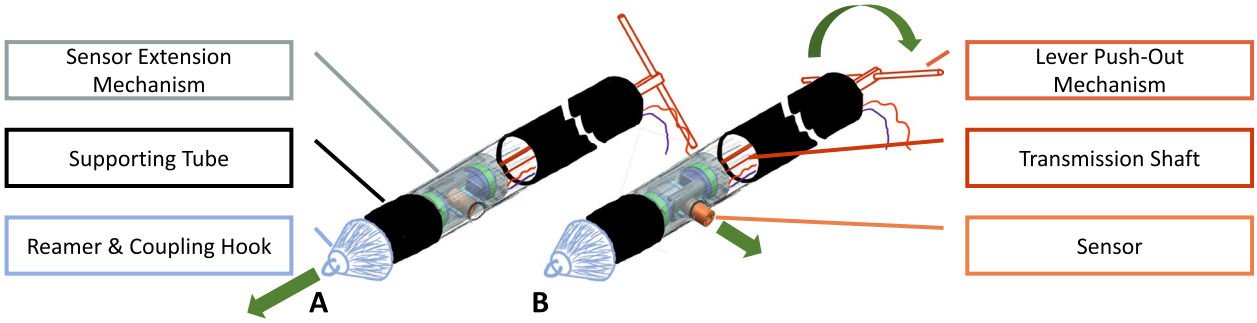

Fig. 3 Concept of the potential mapping in the underground: **A** Electrochemical sensor protected in the supporting tube during the dragging through the underground and **B** After turning the lever, the sensor is pushed out from inside the tube towards the underground, and the measurement procedure is started; after the measurement, the sensor goes back to the initial position in the case. The direction of the green arrows shows the turning direction of the lever arm and the direction of the movement of the probe

underground corrosion assessment of buried RC parts, such as cantilever retaining walls.

Figure 3 presents the detailed concept of the probe, including the details of how the physical contact between the tip of the sensor with the conductive underground is established. The sensor is a so-called reference electrode of the type copper/copper sulfate (see also section 2.3). The HCP mapping permits the assessment of the corrosion state of the steel reinforcement. This non-destructive testing (NDT) method needs to sample points at regular intervals of 15 cm to 50 cm on RC [16–18]. A suitable extension mechanism is essential for contact with the conductive soil/backfill and protection during the transport of the sensor between the measurement points at regular intervals. In our design, an ordinary outer tube protects the underground inspection probe during the dragging through the underground after the pilot drilling by the horizontal drilling machine close to the backside of the wall at the height of the construction joint. This outer tube protects all necessary cables for the HCP measurement.

The pilot drilling connects two excavations at the beginning and the end of the cantilever retaining wall. A coupling hook and a reamer connect the protection tube with the underground inspection probe with the horizontal drilling machine in one of the two excavations (Fig. 3 A). The horizontal drilling machine pushes or pulls the supporting tube through the micro-tunnel in a controlled way. The extension mechanism (detail see section 3.2) pushes the sensor out at discrete locations to acquire a data point as soon as the tip of the sensor is in physical contact with the underground (Fig. 3 B). The working principle of the push-out mechanism is mechanically simple; by turning the lever, the rotational movement is forwarded to the probe, which is transformed into a linear movement to push the sensor out. A turn in the opposite direction returns the sensor into the protection tube.

Probe engineering

The diameter of the horizontal micro-tunnel depends on the backfill material behind the retaining wall. Consequently, the horizontal drilling technology determines the geometry of the supporting tube and the maximal diameter of the underground corrosion inspection probe. In contrast, the length of the probe in the longitudinal direction will be less critical. The conditions of the underground for the field experiment (see section 3.2) led to an outer diameter of 100 mm for the supporting tube and an inner diameter of 72 mm in order to connect to the horizontal drilling machine by a reamer and a coupling hook (see Fig. 3). The resulting gap of at least 9 mm (thickness of the supporting tube) between the tip of the sensor (Details about the sensor in section 2.3) and the underground must be covered by an extension mechanism to enable physical contact with the underground with the tip of the sensor that will be placed inside in this tube. The extension mechanism consists of the following basic mechanical elements: two axial bearings, two groove ball bearings, two rotations disks, two guidance bars, and a pusher. Figure 4 gives an overview of the design of the inspection probe with the individual parts where the sensor is protected in the probe (Fig. 4A) and in Fig. 4B, where the extension mechanism pushes out the sensor. The extension mechanism transforms the rotational movement into a linear motion of the pusher bar by turning the rotation disk 90° from the outside with connectable, square-headed 2 m long steel bars placed inside the tube until the probe, as schematically shown in Fig. 3. Groove ball bearings supported the two rotation disks, and two axial ball bearings guided the pusher bar movement to minimise friction. The linear motion of the

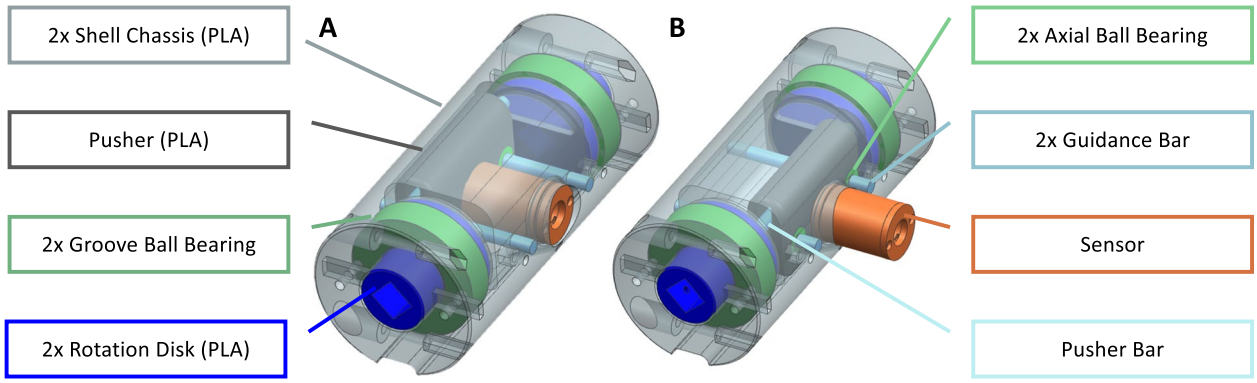

Fig. 4 Overview of the sensor push-out mechanism stored in the tube (without the protection tube): **A** Sensor inside the tube and **B** Sensor pushed out against the environment after turning the rotation disk by 90°

pusher with the centrically placed sensor bar of 30 mm enables direct contact with the tip of the sensor with the underground through an additional hole in the supporting tube. The circular cross-section of the sensor (see also Reference electrode section) was chosen to minimise the gap between the sensor and the open space to avoid the ingress of dirt through the opening if the sensor is pushed out against gravity. Most of the components of the sensor were printed with Polylactide (PLA) with an Ultimaker 2+ 3D printer, and the probe was fixed with two screws to the supporting tube during the field experiment (see Field test section).

Reference electrode

The sensor for the HCP measurement is a so-called reference electrode (RE), which usually is a copper/copper sulfate electrode (CSE) for civil engineering applications. Those sensors typically consist of a plastic container filled with saturated copper sulfate solution, in which a blank pure copper rod is located. Plastic containers offer advantages over glass containers for field applications, such as robustness [19]. A porous plug, also known as the diaphragm, typically made of wood, ensures electrolytic contact to the concrete pore system or, in this application, over the conductive soil to the retaining wall made of RC. The electrolytic contact permits the measurement of the potentials of the reinforcing steel, which is generally done with the help of a voltmeter with a high input impedance and allows obtaining information about the state of corrosion.

The HCP mapping is a well-known NDT method for detecting ongoing macro-cell corrosion in RC and is regulated by several international guidelines [16, 18, 20]. However, suppose such a RE is used for out-of-sight measurements in a rough underground. In that case, it might not be apparent whether the potential readings are still accurate. Possible malfunctions can be caused if the sensor is mechanically damaged, sufficient electrolytic contact is not ensured, or if the electrical circuit is not closed. For typical applications on RC, the contact with the RE on the concrete surface is ensured by a human operator/technician who controls the contact force and detects malfunctions often immediately and visually, such as, e.g. leaking of the solution. To solve the challenge of the out-of-sight measurement, the design of conventional, commercially available CSE is adapted to determine the electrical resistance of the sensor with the stainless steel wire in order to detect malfunctions. High electrical resistances between the rebar and the RE were found to influence the HCP measurement [19], and continuous tracking of the electrical resistances overcame this limitation.

Figure 5 depicts the individual parts of the tailor-made RE adapted for out-of-sight measurements and to fit into the constrained space inside the tube. Consequently, no commercial product could be used for this application. The main body of the RE consists of a thermoplastic Polyoxymethylene (POM) cylinder (Fig. 5 Nr. 7) with a length of 50 mm and an outer diameter of 25 mm with several holes of varying diameters. Compared to a commercial RE, the main modification was the additional stainless steel wire (Nr. 4) through the sponge (Nr. 3) at the tip of the electrode that allows for determining the internal resistance of the sensor. This wire allows measuring the electrical resistance between this wire and the copper spiral (Nr. 8) inside the saturated copper sulfate solution (Nr. 9) over the wooden dowel (Nr. 5). Suppose the RE gets damaged at any time during an inspection, and the solution drips out. In that case, the electrical resistance will increase by several orders of magnitude compared to the fully functional state of the sensor. Consequently, the electrical resistance indicates whether the sensor

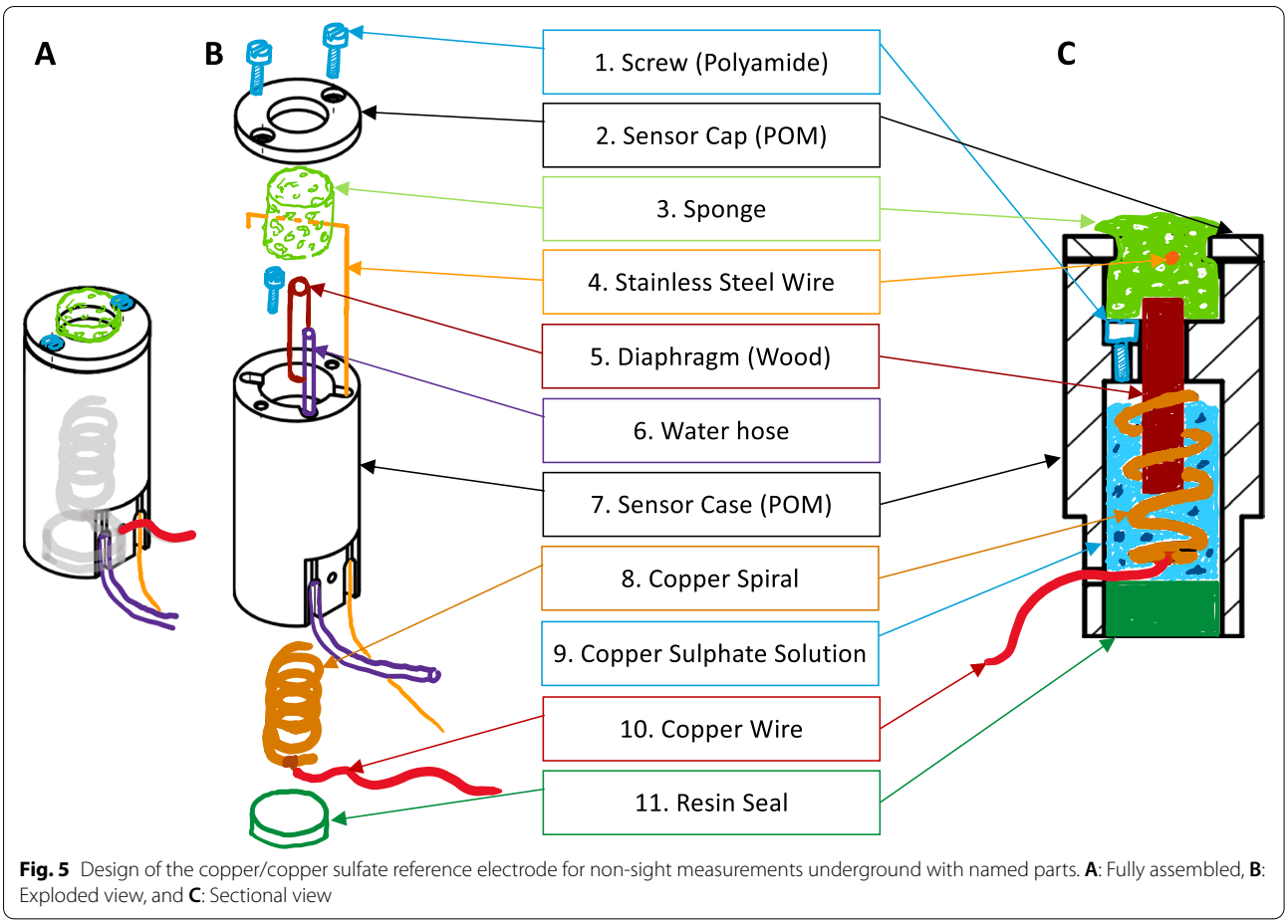

Fig. 5 Design of the copper/copper sulfate reference electrode for non-sight measurements underground with named parts. **A**: Fully assembled, **B**: Exploded view, and **C**: Sectional view

is working or damaged. The wooden dowel ensures the electrolytic connection to the solution at any sensor orientation with respect to gravity since the orientation of the sensor is expected to change during the dragging because of the friction between the outer protection tube and the underground. In addition, this internal resistance is used to correct the electrical resistance measured from the copper spiral to the steel in the structure to obtain an estimate of the electrical resistance between the sensor and the reinforcement in the concrete at any orientation in the underground. This measurement type also gives an indication of the conductivity of the backfill material.

The sponge (Nr. 3) in the sensor head was kept moist by a water tube (Nr. 6) with an outer diameter of 3 mm and an inner diameter of 1 mm. The electrolytic contact with the underground surface is ensured by pumping a conductive electrolyte into the sponge that has a diameter of approximately 12 mm and equals the contact area with the underground. Here, as an electrolyte, we use local tap water with an electrical resistivity of approximately 0.37 Ω·m measured with a SevenExcellence device from Mettler Toledo at room temperature. The sensor cap (Nr. 2) on top of the RE was designed as a wearable part because of the repetitive mechanical contact with the underground (mix of earth, stones, sand, etc.) and fixed with two polyamide screws (Nr. 1) to the main part of the sensor (Nr. 6). The lower end of the sensor was sealed with a two-component resin from the supplier Technovit (Nr. 11) during assembly after the copper spiral, and the copper spiral (Nr. 8) were placed. The saturated copper-sulfate solution can be refilled for maintenance of the sensor through a channel below the sponge with a syringe without the need to disassemble the complete pushing-out mechanism of the probe in the supporting tube (see Fig. 4). This channel is closed during measurements by a polyamide screw (M2.5) and a plastic O-ring for sealing.

Figure 6 shows the fully assembled prototype of the probe head before its insertion into the outer supporting tube connected to the external pusher bar mechanism on the right. The probe head was extended with an additional 3D-printed part that integrates a peristaltic pump and a water reservoir of 0.5 l (plastic bottle) for the field experiment. The additional tap water supply ensured

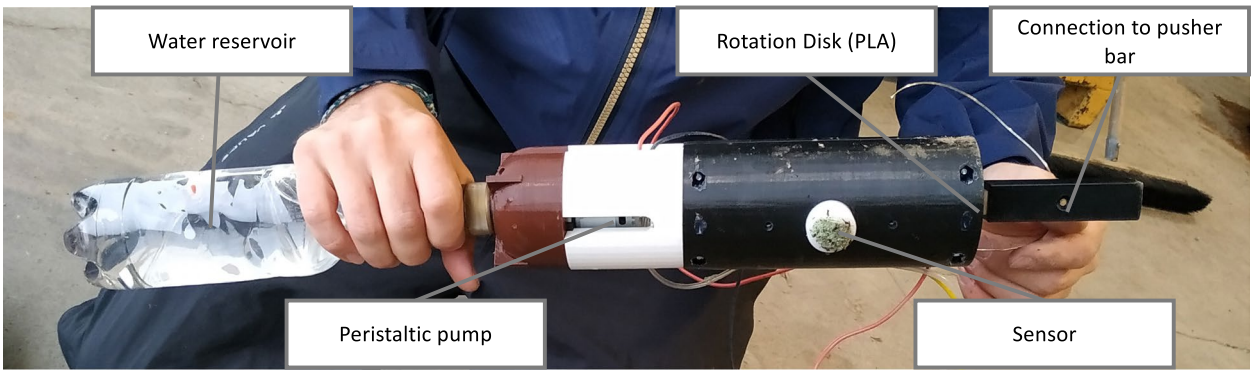

Fig. 6 Assembled prototype of the probe head for the field experiment with the peristaltic pump and the PET bottle as a water reservoir before the insertion in the protection tube

the electrolytic coupling, especially in contact with dry soils or after a high internal resistance of the RE was registered.

Experiments

The experimental part is divided into two parts. The first part includes experiments in the laboratory to 1) check the functionality of the probe and 2) study the detection of local anodes as a function of the distance between the RE and the steel reinforcement compared to measurements on RC. The second part presents the results from the trial of the system on a field site with a horizontal drilling machine and a galvanic cell to mimic the corrosion process in the underground with two types of metal bars.

Laboratory experiments

The influence of various material compositions in the underground in combination with the detection limit of the HCP mapping is still an open question. To better understand how the distance and the resistivity of the soil/concrete play a role in influencing the HCP value, a tailor-made laboratory setup was built. The setup consists of a reinforced mortar block with an artificially introduced localised corrosion spot. The local anodic zone was created by adding sodium chloride at a specific location to the fresh concrete (over a length of approximately 10 cm, see next section for details). The mortar block was placed in a wooden frame in order to allow varying distances via adjustable spacers between the RE and the mortar block. Figure 7 gives an overview of the setup with the wooden frame and the position of the individual measurements along the reinforced mortar block and its dimensions. The gap between the mortar block and the measuring spot was filled with different soil substitutes, such as sand or fine gravel. Afterward, the HCP values were measured in two rows parallel to the mortar block with the tailor-made RE, which was placed in the holes in the wooden frame to allow for contact between the probe and the soil (Fig. 7). Each line consists of 15 potential measurements with a spacing of 50 mm between the contact points and electrical resistance measurements between the RE and the steel reinforcement at each location.

Reinforced mortar block

A mortar block with the dimensions $w \times h \times l = 61\,\text{mm} \times 150\,\text{mm} \times 800\,\text{mm}$ was cast using ordinary Portland cement with water to binder ratio of 0.45. Each of the two reinforcement bars B500B ($\varnothing = 6\,\text{mm}$) was covered with a mortar cover of 20 mm towards the filling material and a cover of 35 mm for the upper bar, respectively. The steel bars were horizontally positioned in the mould during the casting. The artificial corrosion spot was located approximately 550 mm apart from one end of the sample. The localised corrosion was triggered by manually adding sodium chloride as a solid during the casting added after each layer of concrete over a length of approximately 100 mm, resulting in approximately 2% chloride per concrete weight. The mortar block was stored in a climate chamber (20 °C, RH 95%) after casting, before and after each measurement.

Wooden frame

For the experimental part in the laboratory, the mortar block was placed in a wooden frame to ensure a fixed and reproducible distance from the mortar surface of the mortar block with adjustable wooden spacers. The inside of the wooden frame was covered with plastic foil for electrical insulation. The frame allows a distance of up to 320 mm from the mortar surface. The mortar counterpart was a wooden part with two rows (lower and upper

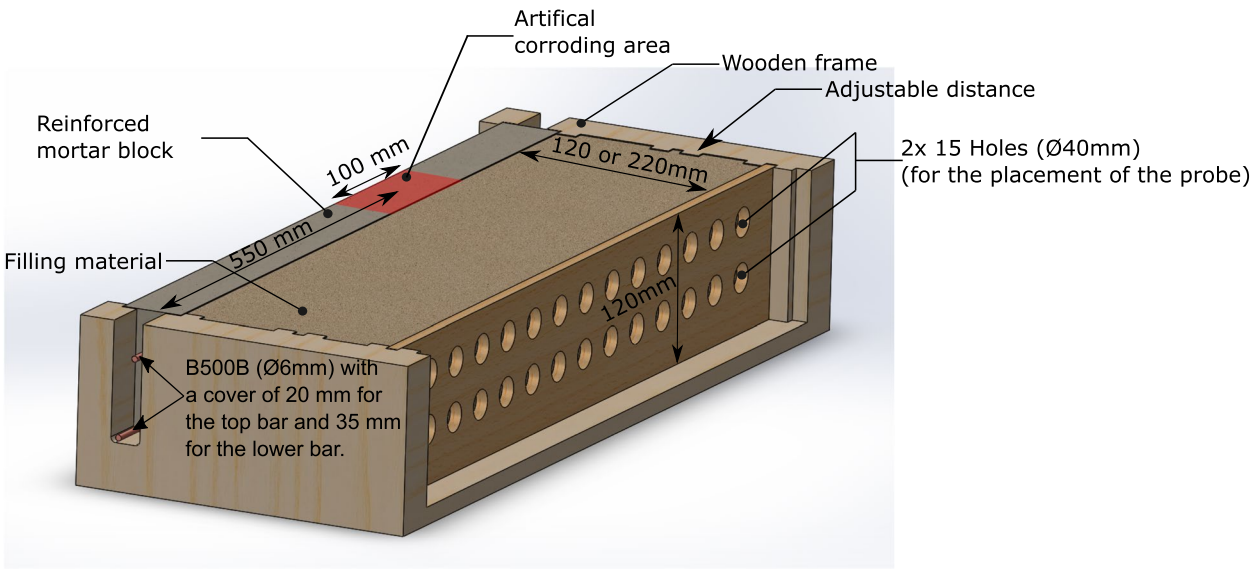

Fig. 7 Sketch of the laboratory setup with the adjustable distance between the mortar surface and the position of the reference electrode indicated by two rows of 15 holes (Ø = 40 mm) and the location of the artificially introduced corrosion location on the reinforced mortar block with two steel bars B500B and its dimensions

row) of each 15 holes (Ø = 40 mm) slightly larger than the diameter of the probe. The holes were covered inside with a fabric to keep the filling material in the wooden frame. The filling material between the mortar block and the counterpart was either sand (0–4 mm) or fine gravel. The distance between the mortar sample and the sensor was either 120 mm or 220 mm apart, with a layer height of approximately 120 mm.

Measurement procedure

Once the block was in position, the measurement protocol consisted of a potential measurement with a digital multimeter (UNI-T UT61 D, input impedance of 3000 MΩ for the mV range) and an LCR-Meter (BK-Precision 879B) for electrical resistance measurements. Both devices were connected for logging purposes to a laptop. The two steel bars were externally electrically connected with a banana plug before the measurements through a hole in the steel (Ø = 4 mm). The potential and the electrical resistance were measured in each hole horizontally from left to right, top to bottom. Potentials were registered for 5 s per point and averaged for further analysis. The electrical resistance between the probe and the steel reinforcement was measured with a frequency of 120 Hz and an amplitude of 600 mV_{rms}. The handheld device was selected as it is considered more suited than a laboratory potentiostat/galvanostat (see the following section) for a field experiment due to the size and the batteries and therefore chosen for this application. The sand or the gravel was slightly kept moist by adding tap water to the sand or gravel after each measurement cycle was finished to maintain a similar moisture state.

The internal resistance of the reference electrode

The internal resistance of the RE was determined by placing the RE in contact with a stainless steel plate and measuring the impedance between the steel and the copper spiral with a fully saturated sponge. The same procedure was used to determine the electrical resistance between the stainless steel wire and the copper spiral for comparison. The internal impedance was measured with a Methrom Autolab PGSTAT302N with frequencies between 10 Hz and 10 kHz and a maximum amplitude of 0.5 V_{rms}. The impedance was measured before and after the experiments on the sample.

Field test

The proof of concept of the developed measuring probe was verified outside of the laboratory situation in a field test. The setup consisted of a galvanic cell formed by electrically connecting eight stainless steel bars and two galvanised steel bars in soil between two excavation shafts. The distance between the two shafts was 6.3 m. The two excavations were connected at a depth of around 70 cm with the help of a horizontally drilled micro-tunnel, where deviations along the planned trajectory were corrected. The micro-tunnel was built in a two-step procedure. The first step was to create a micro-tunnel with a diameter of 80 mm between the excavations with a metallic head. After this head surfaced in the excavation

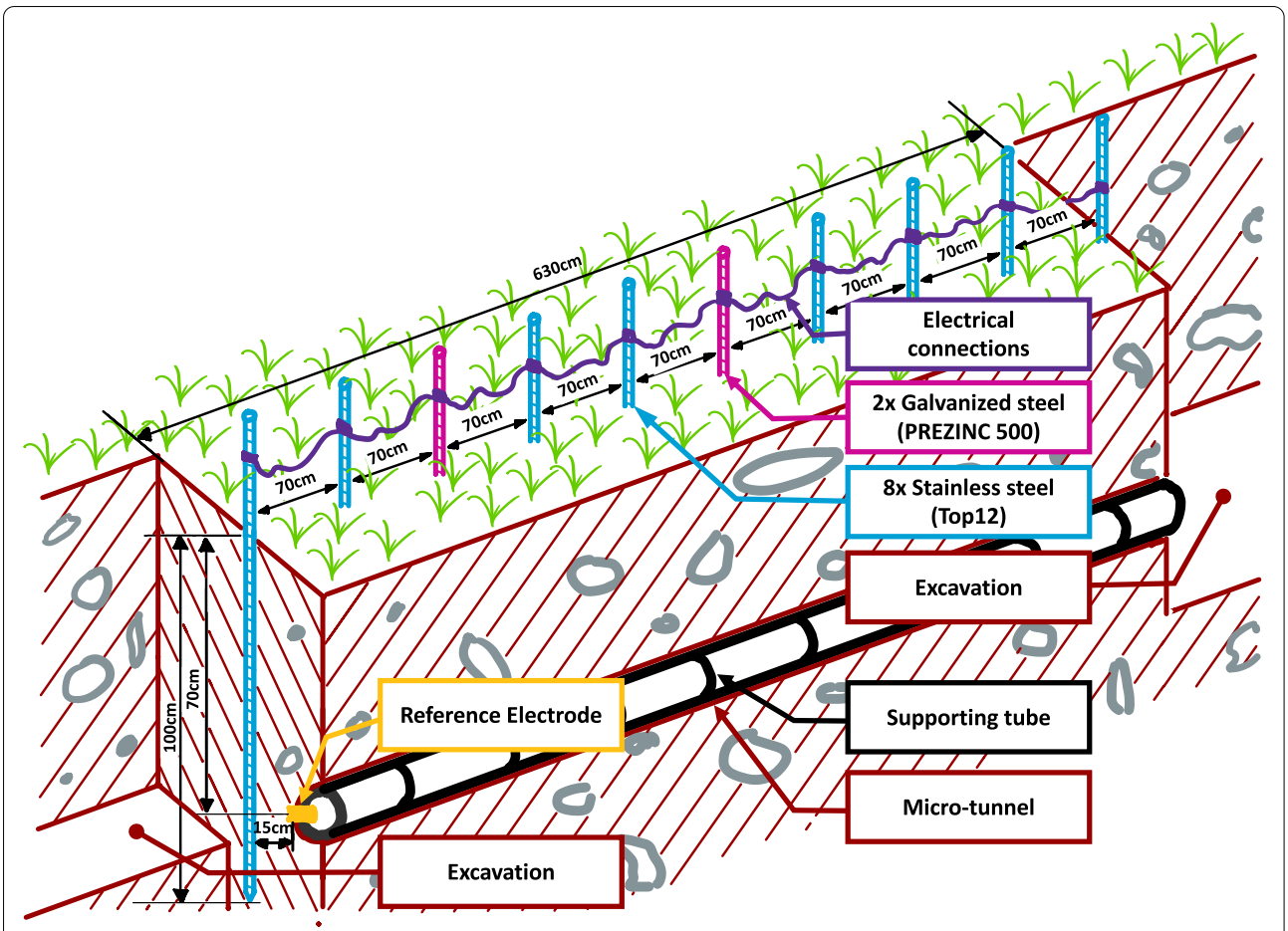

Fig. 8 Setup for the outdoor test of the developed underground corrosion detection system consisting of 10 bars equally spaced 70 cm apart from each other (8 rods 12% chromium steel Ø = 16 mm and 2 galvanised steel rods Ø = 14 mm), which forming a galvanic cell. A borehole was made between two excavations 6.3 m apart from each other at a depth of approximately 70 cm and 20 cm apart from the steels and parallel to them

on the other side, the metallic head was removed and replaced with a reamer (diameter 130 mm) to widen the borehole. The protection tube was mechanically coupled to the reamer and dragged through the underground by a horizontal drilling machine. The underground inspection prototype was fixed with screws at the end of a tube of 10 m in length with an outer diameter of 110 mm. The tube equipped with the prototype was dragged stepwise through the underground with the horizontal drilling machine. At discrete locations at regular intervals of 35 cm, the RE was pushed out against the underground for measurements of the electrochemical potentials and electrical resistances between the sensor and the steels in the soil, as in the laboratory experiments.

Experimental setup

The galvanic cell consists of eight 12% chromium steel (TOP 12) rods with a diameter of 16 mm and two galvanised steel rods (PREZINC 500) 1.5 m in length with a diameter of 14 mm. These rods were manually hammered into the earth perpendicular to the surface up to a depth of approximately 100 cm. The rods were aligned in a straight line between the two excavation shafts. The distance between the rods was 70 cm. Hose clamps attached to a cable electrically connected all steel rods in order to form a galvanic cell in the underground, with the two galvanised steel bars acting as anodes in the system. The two galvanised steels were located 1.4 m and 3.5 m apart from the excavation on the left side (compare Fig. 8). The two excavations were connected with a horizontal drilling machine ("Mini Twinny")[1] approximately 20 cm apart from the middle line of the tube with a gap press technology from right to left (Fig. 8). After the two excavations were connected, the prepared plastic tube (length 10 m) with the probe head was connected mechanically with a

[1] https://www.schenkag.com/mini-twinny/

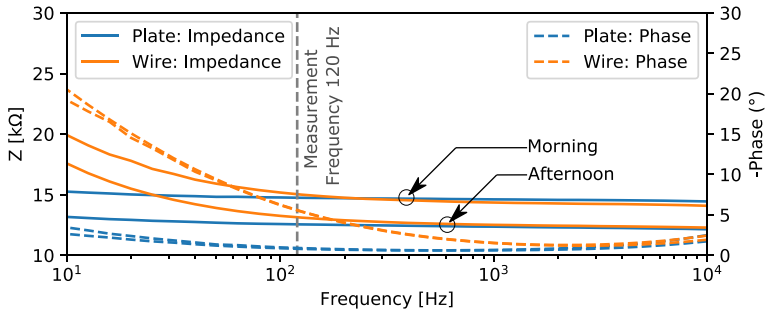

Fig. 9 Impedance and phase angle in dependence on the frequency of the internal resistance of the RE determined while placing the RE on a stainless steel plate or with the stainless steel wire (see Fig. 5 Nr.4) through the sponge at the tip of the electrode

reamer to the horizontal drilling machine to conduct the first measurements during the pullback, controlled by the horizontal drilling machine to the excavation on the left side (left to right in Fig. 8).

The cables for the potential measurement, the electrical resistance measurement, metallic bars for the turning mechanism, and the current cables for controlling the peristaltic pump inside the prototype were placed inside the supporting tube. The internal resistance of the electrode, the resistance between the electrode and the steels before and after pushing-out, and the potential of the steels against the CSE reference electrode were measured at each location. This cycle of measurements was performed at intervals of 350 mm. The acceptance criterion for the registered potential value was that it did not change significantly for a few seconds and was measured with a Fluke handheld multimeter (Model 15B+). The impedance was measured with an LCR-Meter (Escort ELC-131D) with a frequency of 1 kHz and an amplitude of approximately 0.9 V_{rms}.

Results

Laboratory experiments

Sensor assessment

The internal resistance of the RE was determined either on a stainless steel plate or with the stainless steel wire at the tip of the electrode (see Fig. 5 Nr.4). Figure 9 shows the results of the internal resistance and the phase angle of the RE in dependence of the frequency. The internal resistance ranged from 13 to 15 kΩ, slightly changing over time. When measured with the wire, the internal resistance for frequencies less than 100 Hz was higher. However, the internal resistance for frequencies larger than 100 Hz was nearly independent of frequency, and also the phase angle was constantly –of smaller magnitude than 5°. Throughout the measurements, the internal resistance changed moderately. The internal resistance decreased during the experiment in the laboratory, which might have been caused by the additional wetting of the tip and the wooden diaphragm below the sponge at the tip.

Measurements in sand

Figure 10 shows an overview of the results of the potentials in the moistened sand for the measurements in the upper and the lower row in the wooden frame (see Fig. 7). The potentials for a distance of 120 mm from the mortar surface show a clear drop towards where the sodium chloride was added during the casting of the sample and where the location of the anode is expected. The potential drop from the initial measurement on the left side of the block and the lowest measured point was around 150 mV over a distance of 50 cm. The measurements with a distance of 22 cm showed a smaller potential drop and, consequently, a lower potential gradient towards the artificial corrosion spot. However, the potential decrease compared to the nearer distance was reduced to approximately 100 mV. Surprisingly, the potentials at distances over 60 cm from the left end of the mortar block did not increase again for the configuration with 22 cm sand between the RE and the reinforced mortar block. Between the first and the second measurement at a distance of 12 cm, there was a nearly potential drop between the two measurements of approximately 50 mV. This drop might happen due to the interaction at the interface between the moist sand and the mortar block.

The electrical resistance between the sensor and the steel reinforcement did not change while changing the thickness of the sand layer. The electrical resistance was around 1200 kΩ for all measurements and nearly constant for each measured line. A few electrical resistances for the experiment at a distance of 22 cm on the upper row (brown dashed line in Fig. 11) are missing due to an error with the LCR-meter.

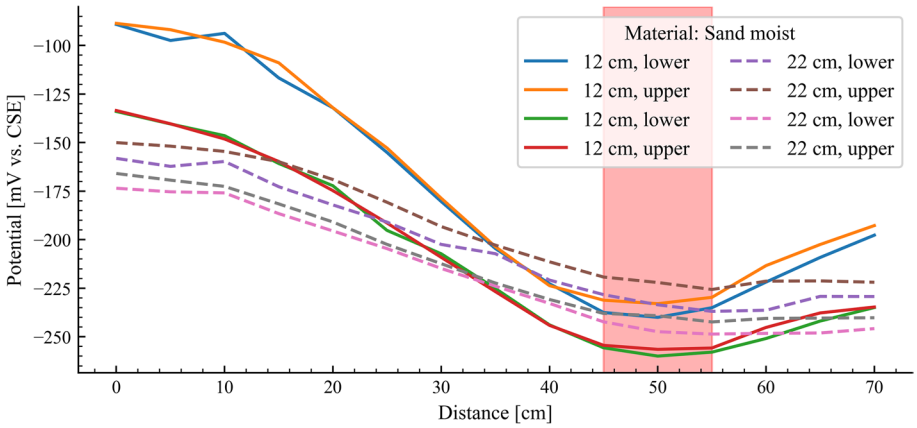

Fig. 10 Comparison of the potential measurement results in moist sand with varying distances between the RE and the reinforcement made of steel for the upper and lower row of holes in the wooden frame (see Fig. 11), where the red rectangle marks the location treated with sodium chloride during the casting of the block

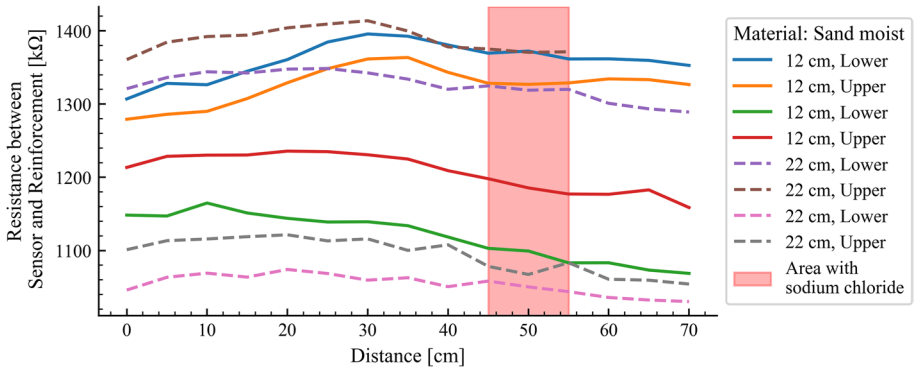

Fig. 11 Electrical resistance between the sensor and the steel reinforcement measured in the wooden frame in the upper and the lower holes (see Fig. 11) filled with sand with varying distances between the sensor and the sample. The red rectangle marks the location treated with sodium chloride while casting the reinforced mortar block

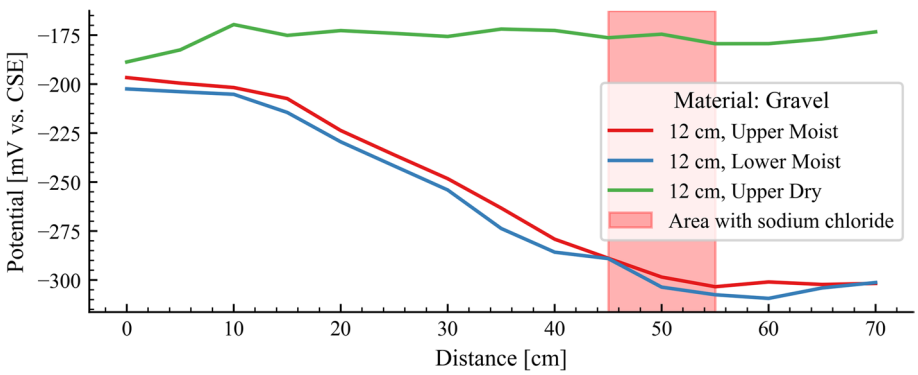

Fig. 12 Comparison of the potential measurement results in dry and moist in dependence on the distance between the electrode and the reinforcement made of steel for the upper and lower row of holes in the wooden frame (Fig. 11) where the red rectangle marks the location treated with sodium chloride

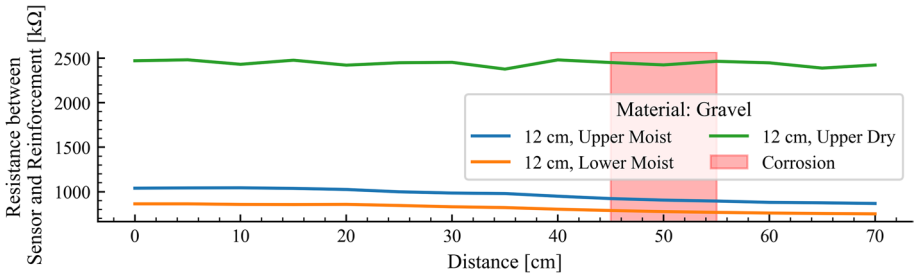

Fig. 13 Electrical resistance between the sensor and the steel reinforcement for gravel as filling material in moist and dry conditions measured with an LCR-meter with a frequency of 120 Hz measured in the upper and the lower row of holes in the wooden frame (see Fig. 11) where the red rectangle marks the location treated with sodium chloride during casting of the sample

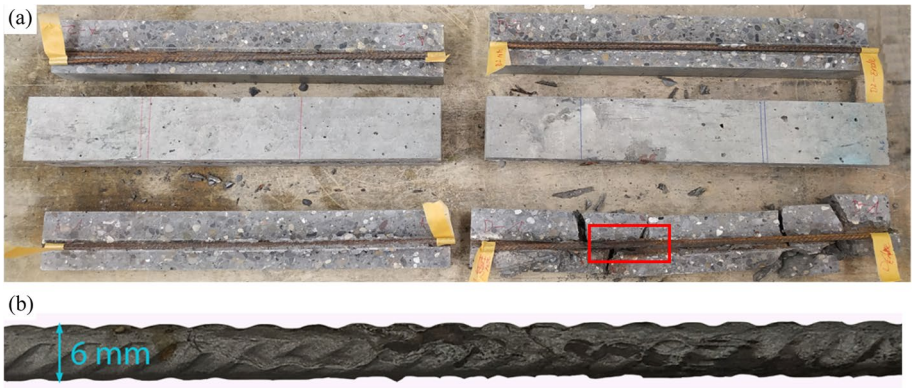

Fig. 14 **A** Splitting the reinforced mortar block with the anode marked with a red rectangle and (**B**) Detailed photo of the reinforcing steel with the anode after sandblasting with the cross-sectional steel loss on the steel with a diameter of 6 mm

Measurement in gravel

Figure 12 shows an overview of the results of the HCP measurements in gravel. The measurement of the upper holes showed that no potential change over the length could be measured for dry gravel. Since similar results were expected for the lower row due to the high electrical resistance, no HCP measurements were executed. The moistened gravel by tap water revealed that potential changes towards the anodic part of the steel were observable as for the measurements in the sand. The experiment showed a potential drop towards the location of the anodic steel part with a decrease of the potential of around 120 mV. The potentials at distances over 60 cm in Fig. 12 did not increase again.

Figure 13 shows the electrical resistance for the lower and the upper row performed in gravel. After some tap water was added, the electrical resistance decreased from 2500 kΩ to around 1000 kΩ, comparable to the resistance measured with sand as filling material (compare Fig. 11). The electrical resistance of about 2500 kΩ for the dry gravel was close to the limit of the measuring range of the LCR-meter. These results shown in Fig. 13 are independent of the coordinate; no changes were observed for locations close to or further away from the mortar part containing chlorides. This observation agrees with the experiments in the sand, where also no drop in the electrical resistance was found in the areas with chloride-contaminated mortar.

Post-experimental assessment of the anode in the mortar block

After finishing all experiments, the spatial extent of the anode was checked by splitting the reinforced mortar sample along the two reinforcement bars (Fig. 7). First, the sample was cut in half perpendicular to the longitudinal axis of the steel bars due to the geometrical limitations of the saw. Afterwards, four notches were cut in order to split the sample parallel to the reinforcing steels. Two notches per piece were cut from the bottom and top of the sample to a distance of about 2 mm from the steel surface. Finally, the two steel bars were uncovered manually with a hammer and a chisel. Figure 14 (b) shows the anode after sandblasting from the red rectangle with visible steel loss in Fig. 14 (a). Only one of the two initially placed steel bars showed visible steel loss, respectively, visual signs of heavy corrosion damage. The anode size

Table 1 Differences between the different measurements with the developed probe during the field experiment

Measurement	*Orientation of the sensor*	*Distance between the tip of the sensor and the reinforcement [cm]*	*Comment*
1	Towards the steel	15	The closest distance between the sensor and the steel reinforcement
2	Upwards against gravity	20	Stress test of the push-out mechanism
3	Towards the steel	15	Repetition of measurement 1

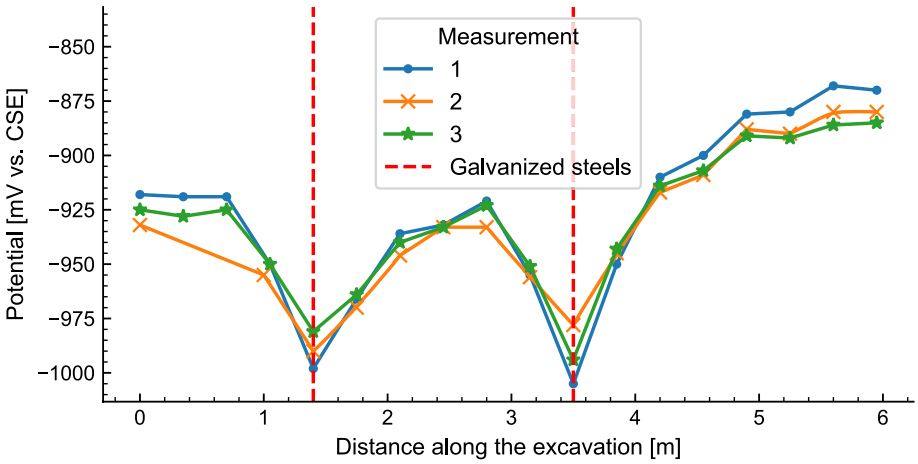

Fig. 15 Result of the HCP mapping with different distances towards the steels with the prototype with the marked locations of the galvanised steels acting as anodes in the electrochemical system during the field experiment

was estimated to have a length of 7.5 cm and started at the coordinate 45.5 cm. This location corresponds with the lower potential measured in sand and gravel (compare Fig. 10 and Fig. 12).

Field tests

Three measurements were performed with the developed probe, whereas two measurements were from left to right, and one measurement was in the opposite direction (compare Fig. 8) with a distance of 35 cm between the measured points. Table 1 summarises the details from the individual measurements with the prototype in the field. The three repetitions with the device had different purposes. The goal of the first measurement was to measure with the closest possible distance between the tip of the electrode and the steel bars because of the findings in the laboratory experiment (see Fig. 10). The laboratory experiments suggested that a higher distance decreased the potential difference between the anodic and cathodic parts. The key idea of the second measurement was to check the robustness of the push-out mechanism by orienting the sensor vertically and pushing it against gravity. This sensor orientation allows for the soil to fall in between the gap between the outer shell of the RE and the tube. The soil material in the gap can cause a malfunction by blocking the push-out channel. The last measurement was an identical repetition of the first measurement to check the repeatability.

The findings of the three HCP line measurements in the soil between two excavations are shown in Fig. 15. All measurements showed a considerable potential drop around the two galvanized steel bars. Furthermore, a gradual decrease from both sides towards both galvanised steel rods was observed. The potential drop was around 100 mV and nearly symmetric around the location of the two galvanised steel bars. In conclusion, the underground inspection system was able to locate the position of the anodes successfully.

Figure 16 shows the electrical resistance between the electrochemical sensor and the steel bars, once when the lever controlling the probe push-out mechanism was in the position where the probe was in the protection tube and once when the lever was turned so that the probe should be pushed out against the underground. The electrical resistance clearly dropped after the push-out. This can be explained by the probe being in contact with the soil when in a pushed-out position (resistance generally of the order of a few kΩ). In this position, the orientation of the probe seemed to be irrelevant. As expected, the electrical contact with the soil was not well defined when

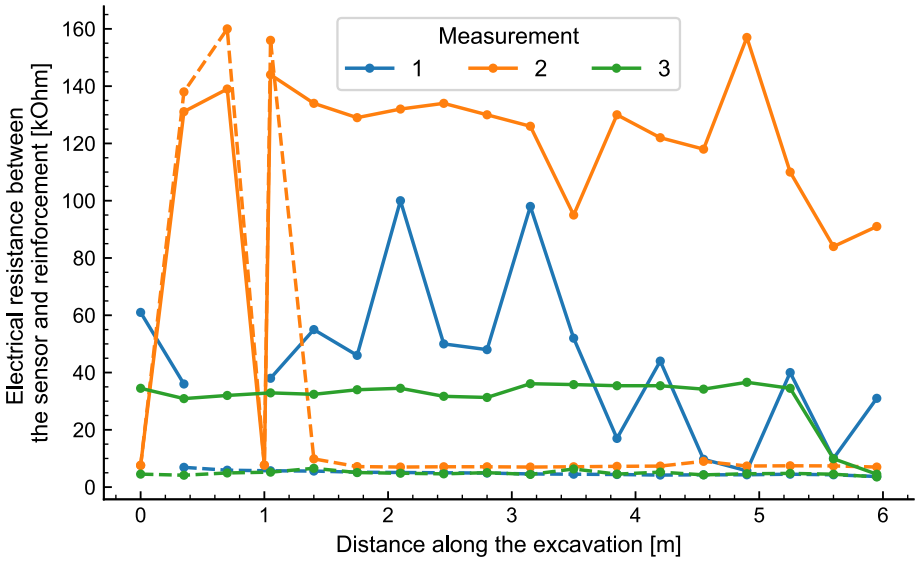

Fig. 16 Result of the electrical resistance measurement at different distances from the steel for the field measurement (all measurements corrected by the internal resistance of the electrode). The colors indicate the number of the measurement (see Table 1). The solid line represents the resistance while the sensor is positioned inside the protective tube, whereas the dashed line represents the resistance when the sensor is pressed against the ground by turning the lever controlling the push-out mechanism

the probe was inside the protection tube. This is reflected by the high and highly varied electrical resistances measured in these cases.

During the second measurement, two potential readings were rejected in the analysis because the resistance did not change substantially, which suggested that the push-out mechanism did not adequately work and insufficient contact between the probe and soil was achieved. For example, at the point at a distance of 1.05 m, this criterion was not fulfilled for the first time since electrical resistance towards the steel reinforcement did not change significantly after turning the pusher bar (144 kΩ and 156 kΩ). An additional point was taken after moving the underground inspection system 5 cm against the measurement direction backward to 1.00 m. The measurement was repeated at this location, and the values had the same magnitude as the previous measurement data at this location (potential and electrical resistance) and were accepted (see also Figs. 15 and 16). The following two potential readings during the second measurement at distances of 35 cm and 70 cm did not show a significant change in the electrical resistance (Fig. 15) and were consequently not taken for further analysis in Fig. 15. However, the last potential reading of this second measurement fulfilled the acceptance criteria. The assumption is that some soil material has covered the distance between the tip of the REF and the soil. This could later be explained by a failure of the connection of the push-out mechanism, which was visually detected after this measurement was finished, and the sensor was accessible in the excavation on the left side (Fig. 8). The cause was a broken connection between the push-out mechanism of the prototype and the metallic tube connected to the external leverage arm. These results show that a functioning push-out mechanism for the underground corrosion detection system is crucial for obtaining valid results. The sensor malfunction was successfully detected out-of-sight due to the additional measurement of the electrical resistance. The broken wooden part was then replaced with a metallic one for the third measurement.

Discussion

Detectability of the corroding zone

The detectability of anodic areas under different conditions depends on factors such as the lateral distance between the probe and the concrete surface, the thickness of the concrete cover, varying soil resistivity, the size of the anode, or the size of the probe in contact with the soil. All these factors ultimately influence the measured HCP and the probability of detecting corroding areas in the underground based on assessing the differences in HCP along the structure.

The laboratory experiments with a different layer of filling material showed that clear potential changes could be measured at distances of 12 and 22 cm from the mortar surface in the soil. The size of the anodes (section 4.1.4) in these experiments can be considered representative of practical conditions [6]. Only the case with the

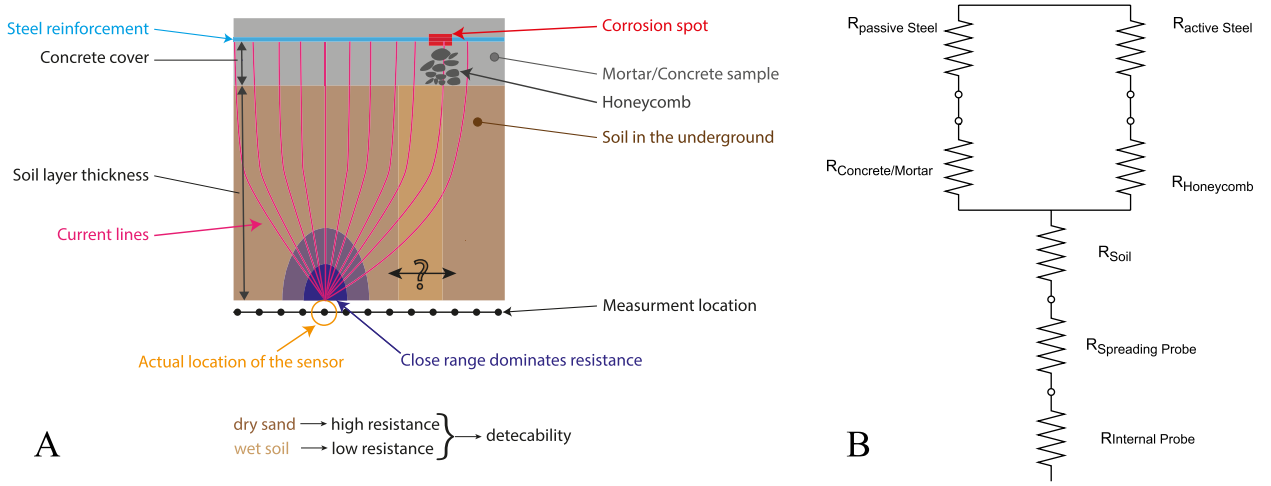

Fig. 17 Possible influencing factors for detecting corrosion of RC members in soil: **A** Sketch of the underground with the reinforced sample and **B** electrical circuit of the underground

highest electrolyte resistance in dry gravel did not show this potential variation over the length of the inspected sample. This may be explained by the fact that under such high resistive conditions, the anodic zone was not actively corroding (because of ohmic limitations of the macro-cell and the lack of moisture needed to promote electrochemical reactions).

The field experiment was designed to assess the feasibility of underground corrosion detection with the HCP mapping outside of laboratory conditions. The results (see Fig. 15) clearly indicate that the galvanised steel acting as anodes in the artificial galvanic cell could be detected at a distance of approximately 20 cm from the location of the steel towards the location of the sensor tip with a clear potential drop of 75 mV vs. CSE. Note that higher distances were not tested and thus, no statements can be made about the detectability at higher distances. It should be mentioned that the combination of galvanized steel bars and stainless steel may not be fully representative of steel bars embedded in concrete. First, the galvanic coupling of stainless steel with galvanized steel bars leads to very negative potentials (around −800 mV vs. CSE). Secondly, the ratio between passive and active parts was different compared to the area ratio in cantilever retaining walls. These factors may have made it less challenging to locate the anode in the field trial compared to conditions of local corrosion in a cantilever retaining wall.

The electrical resistance measurement may provide an additional parameter supporting the detection of local areas with higher risk for corrosion. In general, experience has shown that honeycombs, present at the backside near the construction joint of cantilever walls, correlate with the location of anodes [5, 21]. Therefore, honeycombs may affect the electrical resistivity locally. This spatial variability of electrical resistance, combined with the potential measurements, might enhance the probability of detecting anodic areas in applications on engineering structures. Figure 17 (a) and (b) shows a schematic illustration of the different contributions to the electrical resistance. Since the passive steel in a cantilever retaining wall generally has a very large surface area, its resistance can be considered negligibly small. The resistances attributed to the mortar/concrete, the honeycomb and the soil will depend significantly on the moisture state of these porous materials. In particular, the conditions surrounding the probe strongly affect the spreading resistance of the probe. Furthermore, given the comparatively small probe size, the spreading resistance is expected to be a dominating factor in the entire resistance circuit. Figures 11 and 13 confirm that the moisture condition in the soil and mortar, together with the spreading resistance of the probe is dominating. In these cases, the lower resistivity of the chloride-contaminated concrete compared to the chloride-free concrete is not appreciable in the overall resistance measurement circuit. In addition, Fig. 17 gives an indication that the spread resistance might be dominating the overall resistance between the two electrodes (rebar and probe).

From the present measurements, it can further be concluded that the internal resistance of the used probe lies between 1% and 2% of the Ohmic resistance between the probe and the steel reinforcement. Thus, with the current probe design, the internal resistance of the probe had a negligible effect on the total resistance.

In contrast to laboratory tests, where the sand layer had a homogenous electrical resistivity, the moisture states

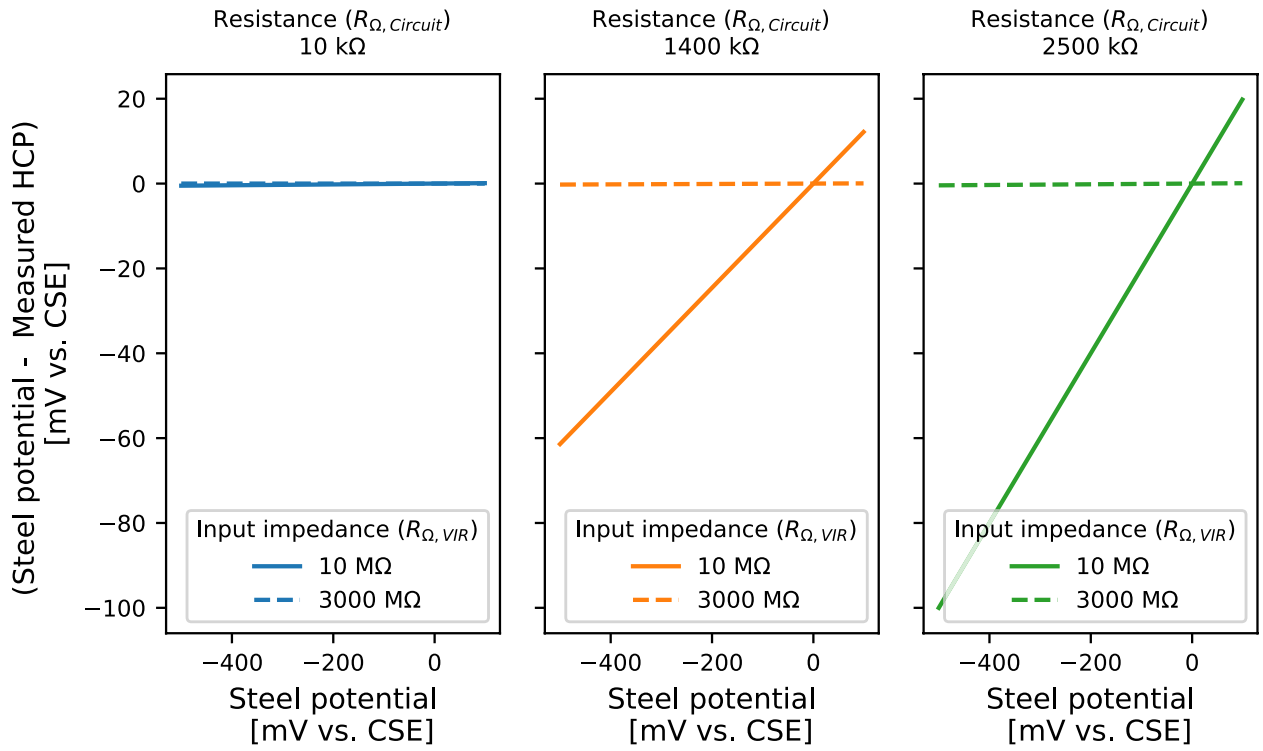

Fig. 18 Evaluation of eq. (1) for several parameter combinations of the input impedance of the voltmeter (10 MΩ. for the solid line and 3000 MΩ for the dashed line) and different resistance of the electrical circuit (10 kΩ, 1400 kΩ, 2500 kΩ)

at the backside of retaining walls may be variable so that zones of higher or lower soil resistivity may be present. Figures 11 and 13 show that it is indeed possible to detect such different moisture states in the soil by employing measurements of the electrical resistance between the probe and the reinforcing steel of the structure.

Thus, we believe that measuring the resistance between the probe and the reinforcing steel provides valuable information complementary to the potential measurements. This can improve the detectability of zones at risk for corrosion.

Effect of the internal resistance of the voltmeter for the half-cell potential measurement

The effect of the circuit resistance ($R_{\Omega, Circuit}$) and the voltmeter's internal resistance ($R_{\Omega, VIR}$) is described by eq. (1) [21]. Eq. (1) was evaluated for several parameter combinations derived from experimental results from this publication and from the equipment in use for the experiments. The evaluation of the different parameter combinations is presented in Fig. 18. The electrical resistance ($R_{\Omega, Circuit}$) from eq. (1) was set to the one of the soil from the field experiment (see Fig. 16) with a value of around 10 kΩ, the contribution of the mortar part and the sand layer with a value of around 1400 kΩ for the laboratory experiment and the second one from the laboratory experiment in dry gravel with an electrical resistance of up to 2500 kΩ. The parameter for the voltmeter internal resistance (input impedance) ($R_{\Omega, VIR}$) was set to 10 MΩ and 3000 MΩ. These values are equal to the input impedance of the digital voltmeter for different ranges for the potential measurement. In addition, the 10 MΩ for the input impedance corresponds to the requirements for applying the HCP technique on RC structures according to the standard in Switzerland [18]. Furthermore, the electrical resistance between the RE and the steel reinforcement must be lower than 100 kΩ for the HCP measurements, according to the SIA Merkblatt 2006 [18] to fulfil the standards for HCP mapping on RC.

$$\text{measured HCP} = \text{steel potential} \cdot \left(\frac{R_{\Omega,VIR}}{R_{\Omega,VIR} + R_{\Omega,Circuit}} \right) \quad (1)$$

Since the results were obtained with an input impedance of 3000 MΩ, the steel potential is very close (error < 1%) to the measured HCP regardless of the electrical resistance of the system (dashed lines in Fig. 18). However, this analysis shows that for underground

measurements, conditions may arise under which the input impedance of the voltmeter is important and should not be too low. Based on our measurements, we recommend an input impedance of 3000 MΩ.

Field application and outlook

Experimental results

The experimental results of the field experiment confirm that probe failure detection with additional electrical resistance measures was functioning. In this way, a defect of the prototype could be determined immediately during the measurement and corresponding precautionary measures and additional functional tests could be initiated. The electrical resistance measurements before and after the pushing-out, combined with the internal resistance of the probe, allowed the detection of a malfunction of the sightless measurement in the underground. The internal resistance of the sensor remained constant in the range of expected values derived from the laboratory experiments (see Fig. 9), while the electrical resistance between the sensor and the steel bars in the soil was not changing significantly.

During the field measurements, the electrical circuit resistance was below 100 kΩ as long as the push-out mechanism functioned (compare Fig. 16). Thus, the consequences of eq. (1) have a negligible influence on the measured potentials.

Future application of the underground inspection prototype

The next development steps in the project will be divided into refinements in the application of the probe in field trials and possible improvements in the detection of corrosion damage through additional measurements on the laboratory scale. Additional NDT methods may further improve the underground condition assessment of cantilever retaining walls or buried structures with a corrosion risk in general.

Soil composition influences the horizontal drilling equipment, which determines the micro-tunnel diameter and limits the bending radius to correct the path. The probe diameter must match the diameter of the micro-tunnel. The probe was also connected in a second excavation for pullback measurements. In applications where access to the structure is limited or traffic obstructions should be avoided, the probe may be integrated into the drilling company's head to avoid the second excavation. Further technological challenges lie in the precise navigation (position and orientation) of the probe during drilling, especially at higher depths or behind RC members where the reinforcement impacts ground-penetration radar (GPR) data. The position and the orientation of the probe could be improved by using accelerometers, as suggested in [22]. However, the design can be adapted to different tube diameters in order to increase the range of applications for underground inspection tasks.

At least three people were required to acquire the results during the field experiment. One person operated the measurement devices and manually switched between cable connections to obtain the results. The second person operated the pusher-bar mechanism, while the last person operated the horizontal drilling machine. We see a potential to automate the measurement further using a robust electro-mechanical push-out mechanism of the sensor, possibly up to a predetermined force threshold combined with automated cable switching and data capturing on a laptop with in-situ analysis and verification of the data.

After several iterations, the sensor design and 3D-printed probe proved robust for the field experiment. Only the wooden connection caused a failure that was replaced on the field trial with a steel connection. Due to higher soil conductivity in the field than in the laboratory, the tap water tube was unnecessary (compare Fig. 11). After the field experiment, the inside of the probe and the inside of the protective tube were checked for incoming soil or underground material. No significant quantities of soil were found at these two locations, and no abrasive damage was found in the vicinity of the sensor. These two observations may depend on soil composition and moisture state. In future experiments, this finding may not apply to other soil compositions. Nonetheless, the sensor should be carefully checked before the next experiment.

Conclusions

This project aimed at developing a technique and probe for the underground corrosion inspection or RC members focusing on the buried backside of cantilever retaining walls. The detection limit of localized corrosion and the influences of soil properties were examined on reinforced mortar blocks. The probe was tested in an outdoor field trial with a galvanic cell to mimic macro-cell corrosion in the underground. The following conclusions are drawn:

- The design of the current prototype, including the tailor-made RE, allowed the out-of-sight measurement of HCP values of reinforcing steel in the underground. Additional measurements of electrical resistances in the measurement circuit proved highly effective in monitoring the functionality of the HCP measurement probe, especially in checking whether adequate contact between the RE and soil was established at each measurement location.
- Both the laboratory experiments and the field trial suggest that local anodic zones (active steel corrosion) of practice-relevant size can be detected with

the proposed approach for a distance between the RE and the steel surface of at least 25 cm. Larger distances away from the reinforcement were not tested.

- The spreading resistance of the probe dominates the electrical resistance measured between the RE and the steel reinforcement embedded in concrete. Major changes in moisture in the soil material were observed to lead to significantly different resistances. Thus, electrical resistance measurements may provide additional information in detecting areas at high risk for corrosion, namely areas with lower electrical resistance indicating moist soil.
- Regarding selecting a voltmeter for such underground corrosion inspection measurements, we recommend using equipment with an input impedance of 3000 MΩ or higher.

On this basis, it is concluded that the proposed approach may enhance the corrosion inspection of cantilever retaining in the future. A major advantage of the proposed solution is that it considerably exceeds the spatial limitations of existing inspection technology for cantilever retaining walls. While the established methods generally only provide (highly) local information, the here proposed approach is capable of measuring at high spatial resolution along a cantilever wall. However, more research and large-scale experiments are required to fully implement and validate this solution in engineering practice or convince stakeholders about the benefits in the service life of such structures.

Abbreviations

RC: Reinforced concrete; HCP: Half-cell potential; NDT: Non-destructive testing; PLA: Polylactide; RE: Reference electrode; POM: Polyoxymethylene; GP: Galvanostatic pulse; LPR: Linear Polarization resistance.

Acknowledgements

The project would not have been possible without the kind support of the company Schenk AG, which was responsible for the underground drilling. In particular, we like to thank Peter Schenk for the organization and the fruitful discussion and Arsim Ali and Marcin Bogdan for their support during the field experiment. Furthermore, most of the work was part of the Master Thesis of Lukas Bircher under the supervision of Alexis Guanella and Marco Hutter. Their contributions to the successful thesis are kindly acknowledged.

Authors' contributions

Patrick Pfändler (PP); Lukas Bircher (LB); Ueli Angst (UA). All authors contributed to the study's conception. LB and PP conducted the experiments in the laboratory and the field experiment. LB has designed and assembled the tailor-made reference electrode and the push-out mechanism according to the discussed and defined requirements with PP and UA. PP prepared the original draft of the manuscript after a discussion on the content with LB and UA. LB created the visualizations (Figs. 1-5, 7-8). All remaining figures were created during the data analysis by PP. LB and UA supported the data analysis with critical discussions and suggestions for improvements. LB and UA reviewed and commented on the document's first draft and edited parts. UA supervised the entire research and acquired the funding. All authors read and approved the final manuscript for publication in the journal.

Funding

Open access funding provided by Swiss Federal Institute of Technology Zurich The authors are grateful to the Swiss National Science Foundation (project no. PP00P2_194812) and the InnoSuisse Bridge Proof-of-Concept Grant (project no. 203686) for the financial support.

Availability of data and materials

Some or all data, models, or code that support the findings of this study are available from the corresponding author upon reasonable request.

Declarations

Ethics approval and consent to participate

Not applicable.

Competing interests

Not applicable.

Received: 11 August 2022 Revised: 3 November 2022 Accepted: 6 November 2022
Published online: 20 December 2022

References

1. Bertolini L, Elsener B, Pedeferri P, Polder RB (2003) Corrosion of steel in concrete. Wiley
2. Romanoff M (1957) Underground corrosion. U.S, Department of Commerce National Bureau of Standards
3. Costello SB, Chapman DN, Rogers CDF, Metje N (2007) Underground asset location and condition assessment technologies. Tunn Undergr Space Technol 22:524–542. https://doi.org/10.1016/j.tust.2007.06.001
4. Unfall auf der Brennerautobahn: Beton-Mauerteile begraben Lkw BILDER VIDEO, https://www.oe24.at/oesterreich/chronik/tirol/unfall-auf-der-brennerautobahn-beton-mauerteile-begraben-lkw-bilder-video/60160925
5. Rebhan MJ, Vorwagner A, Burtscher SL, Kwapisz M, Marte R (2020) Versuchstechnische Untersuchungen zu Korrosionsschäden an Winkelstützmauern. Beton- und Stahlbetonbau. 115:270–279. https://doi.org/10.1002/best.201900073
6. Ryser M, Kölz E, Steiger A, Schiegg Y (2021) Gefährdungsanalyse bestehender Stützmauern
7. Balbi G (2019) Maintenance of retaining structures on the Swiss motorways and national roads. Geomechanics and Tunnelling 12:523–533. https://doi.org/10.1002/GEOT.201900037
8. Vorwagner, A., Kwapiz, M., Rebhan, M.J., Honeger, C.: Possibilities of damage detection in reinforcement of retaining structures. Bridge Maintenance, Safety, Management, Life-Cycle Sustainability and Innovations - Proceedings of the 10th International Conference on Bridge Maintenaince, Safety and Management, IABMAS 2020. 4009–4015 (2021). https://doi.org/10.1201/9780429279119-549/POSSIBILITIES-DAMAGE-DETECTION-REINFORCEMENT-RETAINING-STRUCTURES-VORWAGNER-KWAPISZ-REBHAN-HONEGER
9. Häfliger, S.;, Kaufmann, W.: Experiments on locally corroded retaining wall segments and their assessment with the Corroded Tension Chord Model. Capacity Assessment of Corroded Reinforced Concrete Structures CACRCS (2020) Proceedings. 52, (2021). https://doi.org/10.3929/ETHZ-B-000527046
10. Balazs F (2016) «Filigrane Stützmauern sind passé» Interview mit Balazs Fonyo
11. Tremblay SP, Karray M, Chekired M, Bessette C, Jinga L (2017) Inspection of the lids of shallowly buried concrete structures based on the propagation of surface waves. J Appl Geophys 136:19–34. https://doi.org/10.1016/j.jappgeo.2016.10.020
12. Rebhan MJ, Vorwagner A, Burtscher SL, Kwapisz M, Marte R (2020) Versuchstechnische Untersuchungen zu Korrosionsschäden an Winkelstützmauern: Forschungsprojekt SIBS. Beton- und Stahlbetonbau. 115:270–279. https://doi.org/10.1002/best.201900073

13. Reban M (2015) Ist-Zustandserfassung und Bewertung bestehender, unverankerter Stützbauwerke [Diplomarbeit]. Institut für Bodenmechanik und Grundbau, TU Graz
14. Rebhan, M.J., Marte, R., Tschuchnigg, F., Vorwagner, A., Kwapisz, M.: Safety assessment of existing retaining structures. 17th European Conference on Soil Mechanics and Geotechnical Engineering, ECSMGE 2019 - Proceedings. 2019-Septe, 1–8 (2019). https://doi.org/10.32075/17ECSMGE-2019-0203
15. Taffe A, Hillemeier B, Walther A (2010) Verifizierung moderner zerstörungsfreier Prüfverfahren an einem Abbruchbauwerk: Zustandsermittlung, Untersuchung und Verifizierung von Messergebnissen an einem 45 Jahre alten Spannbetonbauwerk. Beton- und Stahlbetonbau. 105:813–820. https://doi.org/10.1002/best.201000067
16. Sodeikat C (2010) Merkblatt B3 - Elektrochemische Potentialmessungen zur Detektion von Bewehrungsstahlkorrosion Veröffentlicht vom DGZfP-Fachausschuss für Zerstörungsfreie Prüfung im Bauwesen - Unterausschuss Korrosionsnachweis für Stahlbeton. Beton- und Stahlbetonbau 105:529–538. https://doi.org/10.1002/best.201000043
17. Prepared by B. Elsener with contributions from C. Andrade, J. Gulikers, R. Polder and M. Raupach (2003) RILEM TC 154-EMC: recommendations of RILEM TC 154-EMC: 'electrochemical techniques for measuring metallic corrosion'- half-cell potential measurements-potential mapping on reinforced concrete structures. Mater Struct 36:461–471. https://doi.org/10.1007/BF02481526
18. schweizerischer ingenieur- und architektenverein (SIA): Planung, Durchführung und Interpretation der Potenzialmessung an Stahlbetonbauten. 40 (2013)
19. Fan L, Shi X (2019) Techniques of corrosion monitoring of steel rebar in reinforced concrete structures: A review. Structural Health Monitoring 21:1879–1905. https://doi.org/10.1177/14759217211030911
20. ASTM C876–15: ASTM standard C876. Annual book of ASTM standards. 1–8 (2015). https://doi.org/10.1520/C0876-15.2
21. Gu P, Beaudoin JJ (1998) Obtaining effective half-cell potential measurements in reinforced concrete structures. Construct Technol 18:1–4
22. van Disseldrop, R.: UNIQUE AUTONOMOUS PIPELINE MAPPING SYSTEM : AN OVERVIEW. In: 2nd Pipeline Technology Conference. pp. 1–5 (2007)

Publisher's Note